

## New Fe<sup>III</sup>Zn<sup>II</sup> Complex Containing a Single Terminal Fe–O<sub>phenolate</sub> Bond as a Structural and Functional Model for the Active Site of Red Kidney Bean Purple Acid Phosphatase

Mauricio Lanznaster, Ademir Neves,\* Adailton J. Bortoluzzi, Bruno Szpoganicz, and Erineu Schwingel

Departamento de Química—LABINC—Universidade Federal de Santa Catarina, Campus Trindade, BR-88040-900 Florianópolis—SC, Brasil

Received July 22, 2002

The new heterodinuclear complex [Fe<sup>III</sup>Zn<sup>II</sup>(BPBPMP)(OAc)<sub>2</sub>](ClO<sub>4</sub>) (1) with the unsymmetrical N<sub>5</sub>O<sub>2</sub> donor ligand 2-bis[{(2-pyridylmethyl)aminomethyl}-6-[(2-hydroxybenzyl)(2-pyridylmethyl)]amino-methyl]-4-methylphenol (H<sub>2</sub>BPBPMP) has been synthesized and characterized by X-ray crystallography, which reveals that the complex cation has an Fe<sup>III</sup>Zn<sup>II</sup>(μ-phenoxo)-bis(μ-carboxylato) core. Solution studies of 1 indicate that a pH-induced change of the bridging acetate occurs, and the formation of an active [(OH)Fe<sup>III</sup>-Zn<sup>II</sup>(OH<sub>2</sub>)] species as a highly efficient catalyst under weakly acidic conditions for phosphate diesters hydrolysis is proposed.

Purple acid phosphatases (PAPs) constitute a class of metalloenzymes that contain a dinuclear Fe<sup>III</sup>M<sup>II</sup> (M = Fe, Mn or Zn) in their active sites which are able to catalyze the hydrolysis of a variety of phosphoric acid esters and anhydrides within a pH range 4–7.<sup>1</sup> The purple color of this class of acid phosphatases results from a tyrosinate-to-Fe<sup>III</sup> charge-transfer at about 560 nm.<sup>1b</sup> These enzymes have been isolated from animals, plants, and fungi. Recently, the crystal structures of the kidney bean (kbPAP),<sup>2a</sup> the rat (TRAP),<sup>2b</sup> the rat bone,<sup>2c</sup> and uteroferrin PAPs<sup>2d</sup> have been determined, and their similarities suggest a common mechanistic behavior for phosphate hydrolysis. In the kbPAP (resolution 2.65 Å),<sup>2a</sup> the Fe<sup>III</sup> ion is coordinated by a tyrosine, a histidine, and an aspartate, and the zinc is coordinated by two histidines and an asparagine. The Fe<sup>III</sup>Zn<sup>II</sup> ions are bridged by a monodentate carboxylate group of an aspartate and by a modeled μ-hydroxo group. Terminal aqua and hydroxo ligands, which were also modeled, complete the coordination spheres of the Zn<sup>II</sup> and Fe<sup>III</sup> ions, respectively. It is important to emphasize that the two chemically distinct environments around the Fe<sup>III</sup>

and Zn<sup>II</sup> centers are very likely essential for the catalytic properties of this enzyme. Thus, according to the proposed mechanism,<sup>2a</sup> during catalysis the phosphate group is bound to the zinc ion and oriented/activated by this center in such a way that the terminal Fe<sup>III</sup>-bound hydroxide can selectively attack the phosphorus atom, and the product is formed.

From the preceding information, it seems clear that the use of dinucleating N,O-donor ligands that can induce unsymmetrical metal ligation environments and vacant or labile sites for reactivity is a convenient strategy in the search for structural and functional models for PAPs. Heterodinuclear Fe<sup>III</sup>Zn<sup>II</sup> complexes have been described as models for the active site of kbPAP.<sup>3</sup> However, none of them contain the Fe<sup>III</sup>–O<sub>phenolate</sub> motif which in PAPs is responsible for the visible chromophore<sup>1b</sup> and most probably for the stabilization of the Fe<sup>III</sup> ion, which acts as a strong Lewis acid on a bound H<sub>2</sub>O molecule, giving rise to the formation of a nucleophilic hydroxide ion under acidic conditions.

In this communication, we report the first Fe<sup>III</sup>Zn<sup>II</sup> complex containing a terminal Fe<sup>III</sup>–O<sub>phenolate</sub> bond with the unsymmetrical ligand H<sub>2</sub>BPBPMP<sup>4a</sup> as a structural and functional model for kbPAP. The mixed-valence Fe<sup>II</sup>Fe<sup>III</sup>,<sup>4b</sup> Mn<sup>II</sup>Fe<sup>III</sup>,<sup>4a</sup> and Mn<sup>II</sup>Mn<sup>III</sup><sup>4c</sup> containing the M<sup>II</sup>(μ-OAc)<sub>2</sub>M<sup>III</sup> moiety, with the H<sub>2</sub>BPBPMP ligand, have been already described in the literature.

Complex 1 was prepared by simultaneously adding methanolic solutions of Zn(OAc)<sub>2</sub>·6H<sub>2</sub>O (0.5 mmol) and Fe(ClO<sub>4</sub>)<sub>3</sub>·9H<sub>2</sub>O (0.5 mmol) to a methanolic solution containing the ligand H<sub>2</sub>BPBPMP (0.5 mmol) and NaOAc (1.0 mmol) with

\* To whom correspondence should be addressed. E-mail: ademir@gmc.ufsc.br.

- (1) (a) Vincent, B.; Olivier-Lilley, G. L.; Averill, B. A. *Chem. Rev.* **1990**, *90*, 1447. (b) Antanaitis, B. C.; Aisen, P. *Adv. Inorg. Biochem.* **1983**, *5*, 111. (c) Klabunde, T.; Krebs, B. *Struct. Bonding (Berlin)* **1997**, *89*, 177.  
(2) (a) Klabunde, T.; Sträter, N.; Fröhlich, R.; Witzel, H.; Krebs, B. *J. Mol. Biol.* **1996**, *259*, 737. (b) Uppenberg, J.; Lindqvist, F.; Svensson, C.; Ek-Rylander, B.; Anderson, G. *J. Mol. Biol.* **1999**, *290*, 201. (c) Lindqvist, Y.; Johansson, E.; Kaija, H.; Vihko, P.; Schneider, G. *J. Mol. Biol.* **1999**, *291*, 135. (d) Guddat, L. W.; McAlpine, A. S.; Hume, D.; Hamilton, S.; Jersey, J.; Martin, J. L. *Structure* **1999**, *7*, 757.

- (3) (a) Schepers, K.; Bremer, B.; Krebs, B.; Henkel, G.; Althaus, E.; Mosel, B.; Müller-Warmuth, W. *Angew. Chem., Int. Ed. Engl.* **1990**, *29*, 531. (b) Borovik, A. S.; Papaefthymiou, V.; Taylor, L. F.; Anderson, O. P.; Que, L., Jr. *J. Am. Chem. Soc.* **1989**, *111*, 6183. (c) Albedyhl, S.; Averbuch-Pouchot, M. T.; Belle, C.; Krebs, B.; Pierre, J. L.; Saint-Aman, E.; Torelli, S. *Eur. J. Inorg. Chem.* **2001**, 1457. (d) Albedyhl, S.; Schnieders, D.; Jancsó, A.; Gajda, T.; Krebs, B. *Eur. J. Inorg. Chem.* **2002**, 1400. (e) Machinaga, H.; Matsufuji, K.; Ohba, M.; Kodera, M.; Okawa, H. *Chem. Lett.* **2002**, 716.  
(4) (a) Karsten, P.; Neves, A.; Bortoluzzi, A.; Drago, V.; Lanznaster, M. *Inorg. Chem.* **2002**, *41*, 4624. (b) Neves, A.; de Brito, M. A.; Drago, V.; Griesar, K.; Haase, W. *Inorg. Chim. Acta* **1995**, *237*, 131. (c) Karsten, P.; Neves, A.; Bortoluzzi, A. J.; Strähle, J.; Maichle-Mössmer, C. *Inorg. Chem. Commun.* **2002**, *5*, 434. (d) Neves, A.; Horn, A., Jr.; Lanznaster, M.; Vencato, I.; Bortoluzzi, A. J. Manuscript in preparation.

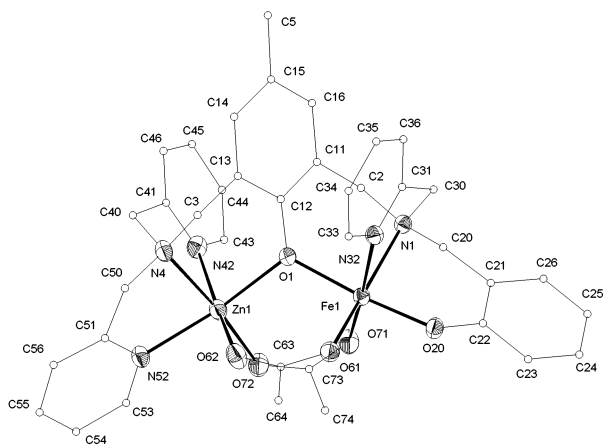


**Figure 1.** ORTEP plot of the cation of **1**. Selected bond lengths (Å) and angles (deg): Fe1–O1 2.006(3), Fe1–O20 1.890(3), Fe1–O61 1.967(3), Fe1–O71 2.034(3), Fe1–N1 2.214(3), Fe1–N32 2.182(3), Zn1–O1 2.105(3), Zn1–O62 2.137(3), Zn1–O72 2.030(3), Zn1–N4 2.185(4), Zn1–N42 2.190(4), Zn1–N52 2.142(3), Fe1···Zn1 3.490(9), Fe1–O1–Zn1 116.22(12).

magnetic stirring at 40 °C for 30 min to yield a dark purple solution. After leaving the solution to stand for a few days at room temperature, a crystalline solid was isolated. Yield: 300 mg, 68%. Anal. Calcd for  $C_{38}H_{39.8}ClFeN_5O_{10.4}Zn$ , fw = 889.62: C, 51.30; H, 4.51; N, 7.87. Found: C, 51.25; H, 4.41; N, 7.82. **CAUTION! Perchlorate salts of metal complexes are potentially explosive and therefore should be prepared in small quantities.** Recrystallization of this sample from MeOH afforded suitable crystals for X-ray structure analysis.<sup>5</sup> The structure and atomic numbering scheme of **1** are illustrated in Figure 1. The molecular structure of **1** shows that in the dinuclear  $[Fe^{III}Zn^{II}(BPBMP)(\mu-OAc)_2]^+$  unit the  $Fe^{III}$  and  $Zn^{II}$  ions are bridged by the phenolate oxygen O1 of  $BPBMP^{2-}$  and by two carboxylate groups of the acetate ligands. The two nitrogen atoms N1 and N32, from the tertiary amine and the pyridine group, and the O20 oxygen of the terminal phenolate complete the  $N_2O_4$  coordination sphere of Fe1. The  $N_3O_3$  octahedral coordination sphere of Zn1 is complemented by the three nitrogen atoms, N4, N42, and N52, of the adjacent bis(2-pyridylmethyl)amine pendant arm of the  $BPBMP^{2-}$  ligand. The average bond lengths around the two metal ions are significantly different as expected for a heterodinuclear mixed-valence species: those around Fe1 average 2.048 Å while those around Zn1 average 2.131 Å. The most obvious differences are found in the distances from the two metal ions to the bridging phenolate oxygen: Fe1–O1 2.006(3) versus Zn1–O1 2.105(3) Å.

The Fe1···Zn1 distance (3.490(9) Å) in **1** is similar to that observed in  $[Fe^{III}Zn^{II}(BPMP)(\mu-OAc)_2]^{2+}$  (3.428 Å)<sup>3b</sup> and also compares favorably to the value of 3.33 Å measured in kbPAP in the presence of phosphate.<sup>2a</sup> The terminal Fe<sup>III</sup>–O<sub>phenolate</sub> bond length (1.890(3) Å) in **1** is also in the same range of those found in the corresponding dinuclear  $[Mn^{II}-Mn^{III}]$ ,<sup>4c</sup>  $[Mn^{II}Fe^{III}]$ ,<sup>4a</sup> and  $[Fe^{II}Fe^{III}]$ <sup>4d</sup> complexes but is

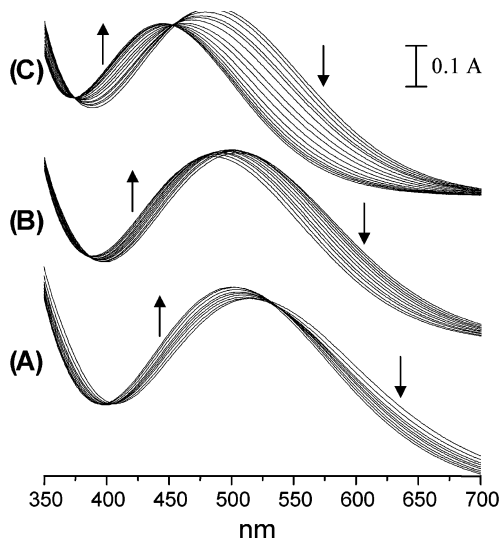


**Figure 2.** UV-vis spectra as a function of pH value: (A) 4.3–5.6, (B) 5.6–7.2, (C) 7.2–10. Addition of 2.0 mol L<sup>-1</sup> NaOH in an ethanol/water 70:30 solution of **1** ( $2.0 \times 10^{-4}$  mol L<sup>-1</sup>) with  $I = 0.1$  mol L<sup>-1</sup> (KCl).

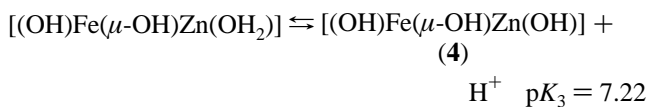
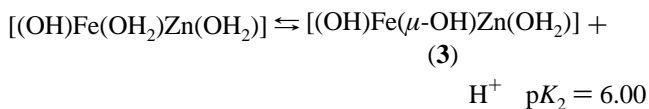
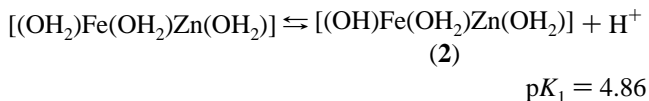
significantly smaller compared to Fe<sup>III</sup>–O<sub>tyr</sub> (2.05 Å) in the native kbPAP enzyme.<sup>2a</sup>

The cyclic voltammogram (Figure S1) of **1** in MeCN/0.1 mol L<sup>-1</sup> *n*-But<sub>4</sub>NPF<sub>6</sub> with scan rate of 150 mV s<sup>-1</sup> reveals one reversible redox process at –910 mV versus Fc/Fc<sup>+</sup> which can be attributed to the one-electron transfer Fe<sup>III</sup>Zn<sup>II</sup>/Fe<sup>II</sup>Zn<sup>II</sup>. This value is in close agreement with the Fe<sup>III</sup>M<sup>II</sup>/Fe<sup>II</sup>M<sup>II</sup> redox couple observed for the Fe<sub>2</sub><sup>4b</sup> (–890 mV) and FeMn<sup>4a</sup> (–870 mV) homologues, respectively.

The electronic spectrum of **1** in MeCN solution consists of a broad band centered at 540 nm ( $\epsilon = 3700$  L mol<sup>-1</sup> cm<sup>-1</sup>), which can be attributed to the terminal phenolate-to-Fe<sup>III</sup> charge-transfer transition.<sup>6</sup> The PAP in red kidney bean shows a tyrosine-to-Fe<sup>III</sup> charge-transfer transition at 544 nm ( $\epsilon = 3200$  L mol<sup>-1</sup> cm<sup>-1</sup>).<sup>1</sup>

Solution studies of **1** (water/ethanol, 30:70) demonstrate that the  $\lambda_{max}$  position of the LMCT process is strongly dependent on the pH of the solution. In the pH ranges 4.3–5.6 (Figure 2A), 5.6–7.2 (Figure 2B), and 7.2–10 (Figure 2C), strict isosbestic points can be observed indicating the presence of only two species in equilibrium, during each individual spectral change. From the distribution curves obtained by fitting the absorbance values versus pH (Figure 3), we propose the following equilibria:

The dissociation of the bridging carboxylate groups of **1** in aqueous medium is quite in line with its well documented



(5)  $C_{38}H_{39.8}ClFeN_5O_{10.4}Zn$ , fw = 889.62, monoclinic,  $P2_1/c$ ,  $a = 19.612(4)$  Å,  $b = 10.795(2)$  Å,  $c = 20.807(4)$  Å,  $\beta = 116.67(3)^\circ$ ,  $V = 3936.4(13)$  Å<sup>3</sup>,  $Z = 4$ ,  $F(000) = 1836$ ,  $\mu = 1.110$  mm<sup>-1</sup>, wavelength = 0.71073 Å,  $T = 293(2)$  K, data/restraints/params 6970/100/514. GOF = 1.036, final  $R$  indices,  $R1$  ( $I > 2\sigma$ ) = 0.0439,  $wR2 = 0.1272$ . Largest diff peak and hole, 0.842 and  $-1.069$  e<sup>-</sup> Å<sup>-3</sup>.

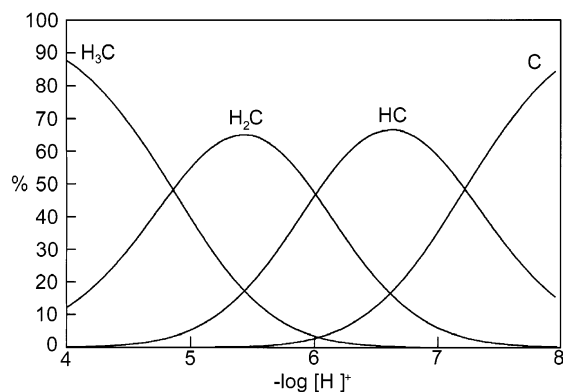


**Figure 3.** Species distribution curves of **1** as a function of pH.  $H_3C$  is the completely protonated species,  $C$  is the completely deprotonated species, and  $H_2C$  and  $HC$  are the intermediate species.

lability,<sup>6</sup> and the 2/3 species are most probably the active species toward the cleavage of phosphate diesters under the same pH conditions (vide infra).

Kinetic experiments to examine the phosphatase-like activity have been carried out with the activated substrate 2,4-bis(dinitrophenyl)phosphate (BDNPP)<sup>7</sup> by following spectrophotometrically the absorbance increase of the liberated 2,4-dinitrophenolate anion ( $\lambda_{\max} = 400$  nm with  $\epsilon = 19100$  L mol<sup>-1</sup> cm<sup>-1</sup>), under conditions of excess substrate. To take into account the spontaneous hydrolysis of the substrate, correction was accomplished by direct difference using a reference cell under identical conditions without adding the catalyst.

The pH dependence of the catalytic activity between 3.63 and 10.00 shows a bell-shaped profile (Figure 4) with an optimum at about pH 6.5. Sigmoidal fits of the curve reveal  $pK$  values at 4.80 and 7.50, which are in good agreement with the values (4.86 and 7.22) obtained from the UV-vis titration experiments. These results strongly suggest that the monohydroxo form of the complex is the active species for cleaving BDNPP, because, as proposed previously, it provides a labile Zn–OH<sub>2</sub> bond for phosphodiester binding and an Fe<sup>III</sup> bound hydroxide group for nucleophilic attack on the phosphorus atom. The decrease in reactivity at pH > 6.5 most probably arises because of the presence of the fully deprotonated form **4** in which the leaving tendency of the OH<sup>-</sup> ion from the Zn–OH group becomes lower, even though a more concentrated OH<sup>-</sup> solution can increase the spontaneous hydrolysis.

The determination of the initial rates at pH 6.1 as a function of substrate concentration reveals saturation kinetics

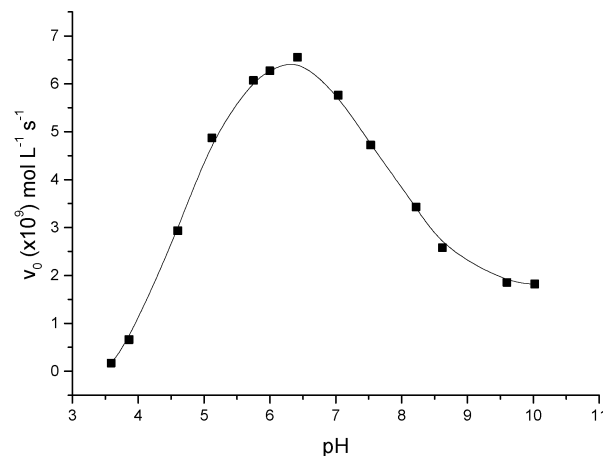


**Figure 4.** Dependence of the reaction rate on the pH, under the following conditions: water/acetonitrile 50% solution,  $[I] = 4.0 \times 10^{-5}$  mol L<sup>-1</sup>,  $[BDNPP] = 2.0 \times 10^{-3}$  mol L<sup>-1</sup>,  $[buffer] = 5.0 \times 10^{-2}$  mol L<sup>-1</sup> (buffer = MES, HEPES, and CHES),  $I = 0.1$  mol L<sup>-1</sup> (LiClO<sub>4</sub>).

with Michaelis–Menten-like behavior (Figure S2). A linearization after Lineweaver–Burke (Figure S3) gives the following values:  $K_m = 8.10 \times 10^{-3}$  mol L<sup>-1</sup>,  $V_{\max} = 2.92 \times 10^{-8}$  mol L<sup>-1</sup> s<sup>-1</sup>, and the catalytic constant  $k_{\text{cat}} = V_{\max}/[I] = 7.31 \times 10^{-4}$  s<sup>-1</sup>. Under these conditions, **1** shows a 4060 times acceleration rate compared to the uncatalyzed hydrolysis ( $k = 1.8 \times 10^{-7}$  s<sup>-1</sup>). To the best of our knowledge, this represents the best model complex so far which hydrolyzes BDNPP.<sup>8</sup>

In summary, we have described the first Fe<sup>III</sup>Zn<sup>II</sup> complex which contains only one terminal Fe<sup>III</sup>–O<sub>phenolate</sub> bond as a structural model for the active site of kbPAP. Furthermore, it was demonstrated that in aqueous solution the [(OH)FeZn(OH<sub>2</sub>)] species is a highly efficient catalyst in the hydrolysis of phosphate diester, probably through a mechanism similar to that proposed for the enzyme kbPAP. Further studies involving the syntheses of homo- and heterodinuclear M<sup>III</sup>M<sup>II</sup> complexes with the unsymmetric H<sub>2</sub>BPPMP ligand and their interactions with phosphate diester bonds in model substrates and DNA are in progress and will be the subject of future reports.

**Acknowledgment.** Financial support was received from CNPq and PRONEX.

**Supporting Information Available:** X-ray crystallographic details for complex **1** in CIF format. Figures S1, S2, and S3 showing the cyclic voltammogram and kinetics details, respectively, in PDF format. This material is available free of charge via the Internet at <http://pubs.acs.org>.

IC025892D

(6) Lambert, E.; Chabut, B.; Chardon-Noblat, S.; Deronzier, A.; Chottard, G.; Bousseksou, A.; Tuchagues, J. P.; Laugier, J.; Bardet, M.; Latour, J. M. *J. Am. Chem. Soc.* **1997**, *119*, 9424.

(7) Bunton, C. A.; Farber, S. J. *J. Org. Chem.* **1969**, *34*, 767.

(8) Duboc-Toia, C.; Ménage, S.; Vincent, J. M.; Averbuch-Pouchot, M. T.; Fontecave, M. *Inorg. Chem.* **1997**, *36*, 6148.